GENESIS AND GEOGRAPHY
OF SOILS

Cryogenic-Lateral Hypothesis of the Formation of the Parent Rock of Soddy-Podzolic Soils Using the Example of the Ryshkovo Paleosol (MIS 5e) in the Taneyev Quarry, Kursk Region

S. A. Sycheva[a], * (ORCID: 0009-0005-8835-0877), **O. S. Khokhlova**[b] (ORCID: 0000-0002-8989-9395), **E. G. Ershova**[c], **T. N. Myakshina**[b] (ORCID: 0000-0002-0301-864X), and **P. A. Ukrainskiy**[d]

[a] *Institute of Geography, Russian Academy of Sciences, Moscow, 119017 Russia*
[b] *Institute of Physicochemical and Biological Problems of Soil Science, Russian Academy of Sciences, Pushchino, Moscow region, 142290 Russia*
[c] *Faculty of Biology, Lomonosov Moscow State University, Moscow, 119991 Russia*
[d] *Belgorod State National Research University, Belgorod, 308015 Russia*
*e-mail: sychevasa@mail.ru

Abstract—The Ryshkovo paleosol of the Mikulino Interglacial (MIS 5e), Late Moscow loess (MIS 6), and buried small erosional landforms were studied in the Taneyev Quarry of Kursk oblast, in the center of the East European Plain. Macro- and micromorphological and palynological analyses of the soil samples were carried out, and the OSL age and physicochemical properties were determined. The history of erosional landforms, soils, and landscapes was reconstructed on the basis of the facial analysis of the paleosol catena. It was concluded that the differentiation of the paleosol profile into the Ah−E−Bt horizons was developed during the Mikulino Interglacial, whereas the initial heterogeneity of the parent material had been formed earlier, during the Late Moscow (Saalian) Glaciation, under the impact of slope and cryogenic processes. The lithological matrix of the Ryshkovo paleosol did not remain unchanged due to the different history of interaction of eolian and slope (solifluction and colluvial) processes, initial pedogenesis, and interglacial soil formation.

INTRODUCTION

Soddy-podzolic and gray forest soils have texture-differentiated profiles consisting of horizons with contrasting properties: dark gray silty loamy humus-accumulative horizon, light gray sandy loamy eluvial horizon, and brown clay loamy illuvial horizon. For gray forest soils, several transitional horizons are noted: AhE, EB. The genesis of texturally differentiated soils still causes heated debate among soil scientists. There are several hypotheses for the development of a profile with an eluvial horizon depleted of clay and sesquioxides and an illuvial horizon enriched in these substances. The age of formation of this profile, as well as the age and genesis of the parent rock, is ambiguously assessed.

The main hypothesis is the classical monochronous soil hypothesis, which assumes the formation of a profile from a homogeneous loesslike sediment during the last interglacial—the Holocene—under the impact of several pedogenic processes: soddy, podzolic, eluvial-gley, and lessivage [9, 12, 18, 30]. An excess of physical sand and a significant deficit of clay almost throughout the entire soil profile are noted [29]. At the same time, the total loss of soil mass is less than the deficit of clay. An excess of clay in the Bt horizon as compared with clay removal from the eluvial horizon was found by Rode [18] for the brown podzolized soil.

With the appearance n of extensive paleogeographic data on climate variability in the Holocene and the use of micromorphological and radiocarbon methods, the soil monochronic hypothesis was transformed into an evolutionary polychronous hypothesis explaining the formation of the second humus horizon and the temporal sequence of leading processes (stages of soil formation), but still attributing the textural differentiation of forest soils exclusively to the Holocene; the main phase of textural differentiation, according to researchers, occurred in the last third of the Holocene [2, 4, 5, 17, 40].

A different—lithogenic—hypothesis was proposed by Sokolov [20−22] and Makeev [14]. According to it, the parent rock of texture-differentiated soils represents an initially two-layered sediment formed as a result of the accumulation of light loamy eolian sedi-

ment (Valdai loess) on heavier loams of the Late Pleistocene and even Middle Pleistocene age. This predetermined the formation of a texturally differentiated soil profile in the pre-Holocene time, during the Valdai Glaciation. In the Holocene, only a small modification of this profile took place, which did not significantly change the main physicochemical properties of the texture-differentiated soils [15].

This hypothesis was continued in the hypothesis of lithogenic cycles proposed in [5, 6, 10, 11] and considering the illuvial horizons as residual buried elementary pedogenic formations (EPOs) developed on "fresh" loess sediment in the Late Glacial period. Based on the ideas of these authors, the parent rock of modern soddy-podzolic soils is multilayered, and the textural differentiation of the profile is mainly due to the superposition of the initial late-glacial soils due to the displacement of tectonic blocks, the so-called "keyboard" neotectonics [10]. In the Holocene, only biochemical processes affecting the properties of the surface humus-accumulative and humus-eluvial horizons took place.

In foreign science, particularly, in German geological literature, the concept of slope beds is widely discussed [34, 35, 37]. It was found that slope sediments cover a larger part of gentle mountain slopes in Central Europe. This cover is subdivided into three layers: the widespread upper layer of relatively uniform in thickness; the intermediate layer confined to flat terrain, depressions, and leeward slopes; and the lower or basal layer. The upper and intermediate layers contain redeposited loess. All three cover layers were mainly formed as a result of periglacial solifluction. Based on the dating of ash inclusions, the age of the layers was determined. The upper layer formed during the Late Glacial and possibly during several short episodes of eolian activity in the Early Holocene. In contrast, the underlying layers may be diachronic, but their structure reflects repeated vertical sediment sequences. The intermediate layer was formed during the Last Glacial Maximum (LGM) and redeposited during the Late Glacial. The age of the lower layer is less specific ranging from Saalian II Late Glacial (MIS 6) to MIS 4. The two upper layers served as the parent material for eluvial and illuvial horizons of modern Holocene soils.

These ideas about the genesis and age of covering sediments that served as the parent material for texture-differentiated soils were also applied to other territories with soils of a similar morphology [35].

The differences between the groups of hypotheses for the genesis of sharply differentiated soils, i.e., between pedogenic and lithogenic hypotheses concern the time and mechanism of formation of the soil-forming rock—cover or loesslike loams—and the role of soil formation in the Late Glacial and Holocene.

Similar ideas about the problem under discussion can be applied to analyze the genesis of the parent material of the soils of the previous Mikulino (Eemian) interglacial period—the Ryshkovo paleosol and its analogues. Modern Holocene soils, including soddy-podzolic soils, have not yet completed their entire development cycle. The study of paleosols of the Eemian Interglacial makes it possible to estimate the full interval of soil development during the entire interglacial and thus contributes to our understanding of the evolution of texturally differentiated soils [27].

Long-term studies of the Ryshkovo paleosols have been performed in a number of quarries (Aleksandrovsky, Mikhailovsky, Taneyevsky (Taneyev) quarries) and in other sections. On their basis, a new hypothesis for the formation of texturally differentiated soils under the impact of lateral cryogenic processes (the cryogenic-lateral hypothesis) has been suggested. In this article we rely on the results of studying the Ryshkovo paleosols (MIS 5e) in the Taneyev Quarry, Kursk region.

The purpose of the work is to evaluate the full time and conditions of formation of the parent rock and the profile of texturally differentiated soil using the example of the Ryshkovo paleosol of the Mikulino (Eemian) Interglacial (MIS 5e) in the center of the East European Plain.

OBJECTS AND METHODS

Loess—soil sequences with Ryshkovo paleosol were studied in the walls of the Taneyev Quarry, 25 km south of Kursk (Fig. 1) and 15 km south of the reference section in Aleksandrovsky Quarry. The Taneyev Quarry is located on a watershed between a large balka (ravine) open towards the Reut River floodplain and its small right tributary.

In the Taneyev Quarry the paleocatena along the shallow Moscow—Mikulino paleohollow (the upper reaches of the paleobalka) from the upper part of the slope of northern exposure to the bottom (Fig. 2) was studied. Soil pits 1, 2, and 3 with the Ryshkovo paleosol were excavated in the bottom of the paleohollow. Soil pit 4 was located higher, upslope from the bottom.

Macromorphological descriptions of soil profiles were made; soil samples, including undisturbed samples for preparation of thin sections, were taken from the horizons and layers described in pit 3.

Laboratory analyses included the determination of the total carbon content (C_{tot}) by Tyurin's method modified by the authors [7]; the amount of CO_2 released during oxidation was determined on a chromatograph; the CO_2 of carbonates was determined manometrically based on the pressure difference in the control and in the sample placed in sealed vessels with rubber stoppers, in which the samples reacted with 10% hydrochloric acid. The results were recalculated to C (C_{carb}). The organic carbon content (C_{org}) was calculated by subtracting C_{carb} from the C_{tot}. Particle-size distribution was studied using the pipette
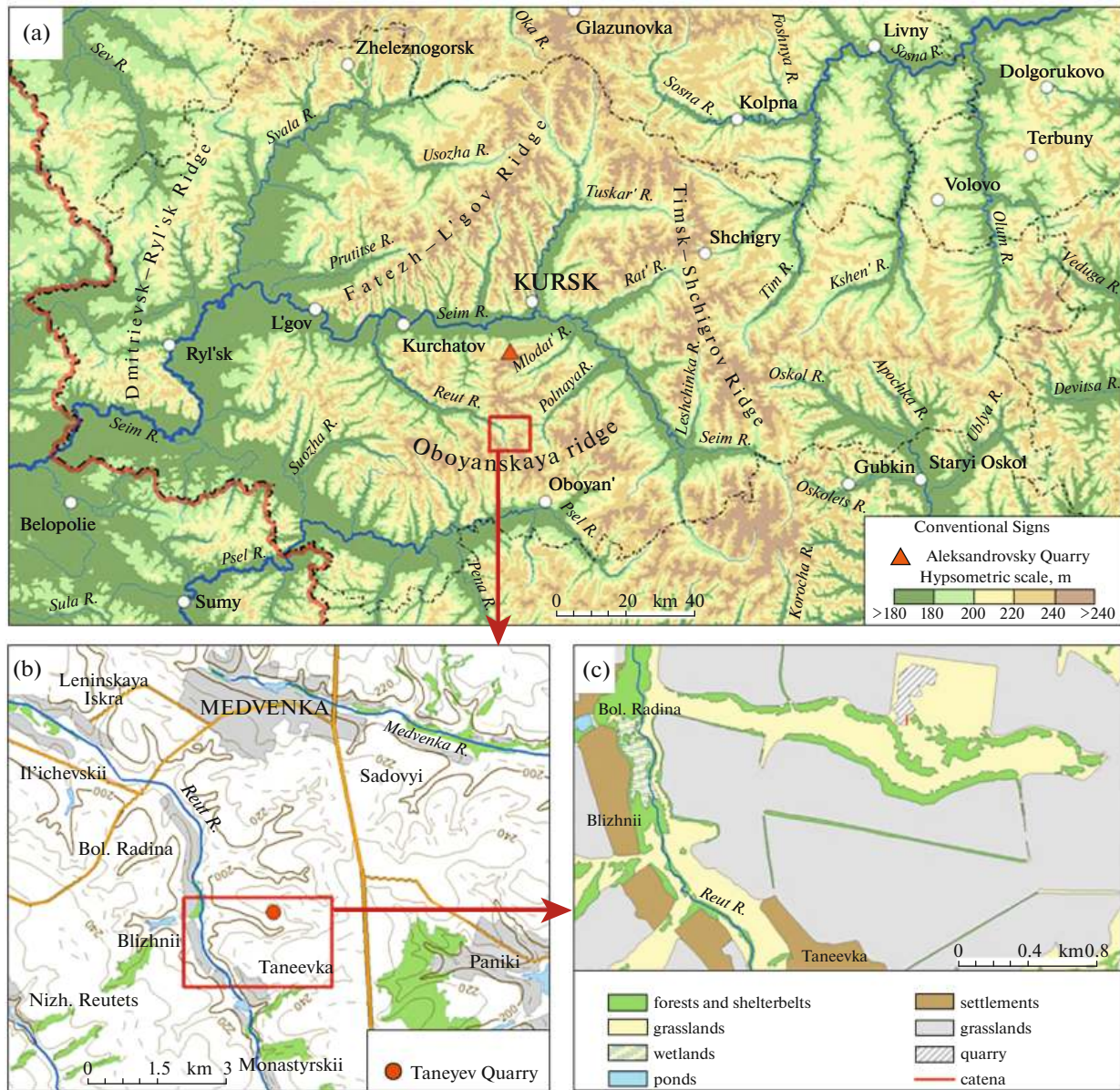
Fig. 1. Location of the Taneyev Quarry on the maps of (a) Kursk region, (b) local topography, and (c) landscape position.

method with pyrophosphate pretreatment of the samples; particle-size fractions were calculated per absolutely dry sample weight with due account for the hygroscopic moisture content. Specific magnetic susceptibility (MS) of the air-dry samples was measured in laboratory conditions using a Kappabridge instrument KLY-2 at the Center for Collective Use of the Institute of Physicochemical and Biological Problems of Soil Science (Russian Academy of Sciences) in Pushchino. Micromorphological analysis of thin sections was carried out using an AxioScope microscope A1 Carl Zeiss (Germany) in the same center.

Six samples from humus horizons (0−28 cm) of the Ryshkovo paleosol were taken for the spore-pollen

analysis. In laboratory, 60-g samples were treated with a 10% HCl solution, boiled in a 10% KOH solution, and centrifuged in a heavy liquid (sodium polytungstate). Pollen and spores were counted and identified in preparations under a light microscope.

RESULTS AND DISCUSSION

Morphological analysis. Watersheds in the Taneyev Quarry area are composed of a thick layer of alluvial−marine sands of the Paleogene age overlain by a thin (1−2 m) layer of Pleistocene loess and slope sediments. The thickness of loess naturally increases towards modern erosional landforms reaching 5−6 m or more in the middle part of their slopes. Local peaks
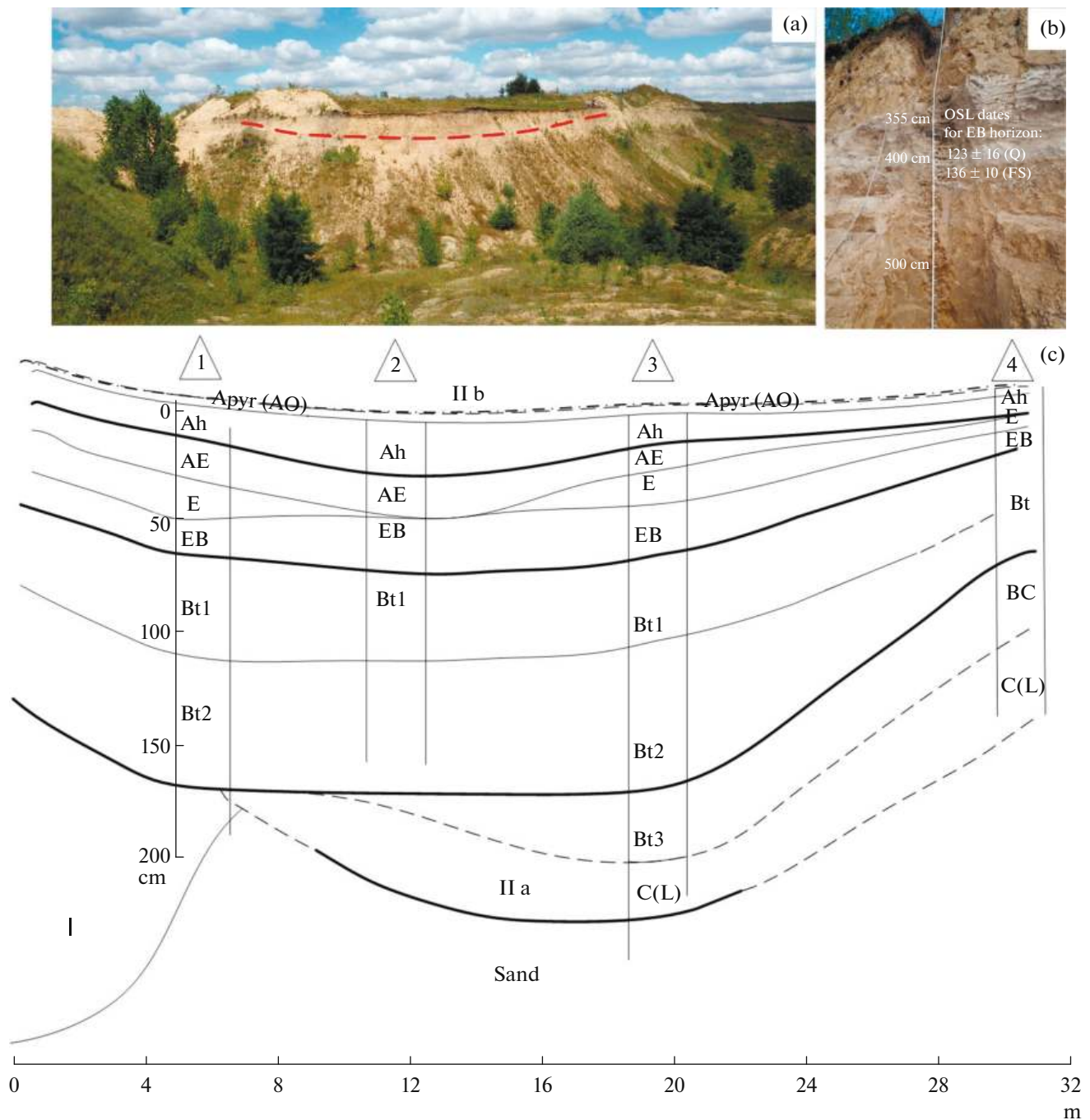
Fig. 2. Buried small erosional landforms (BSEL) and morphology of Ryshkovo paleosols in the Taneyev Quarry: (a) general view of the quarry wall with a preserved fragment of the Moscow−Mikulino paleohollow; (b) pit 3, texturally differentiated soil MIS 5e with OSL dates for quartz (Q) and feldspars (FS); (c) paleocatena. Roman numerals on (c) indicate the stages of BSEL formation: (I) Late Moscow periglacial ravine, (IIa) Late Moscow Glacial paleohollow, (IIb) Interglacial Ryshkovo depression. At the top, numbers of soil pits are indicated in Arabic numerals in triangles. The lines indicate the boundaries of layers (bold) and horizons and subhorizons; dotted lines—estimated boundaries.

in the loess thickness are characteristic of the buried small erosional landforms (BSELs) exposed in the wall of the quarry.

On the north-facing slope of one of such landforms— periglacial ravine I—the Late Moscow−Mikulino shal- low paleohollow IIa was identified (Fig. 2c). This paleohollow is filled with pale yellow loesslike loam (Late Moscow (Saalian) loess) with a lens-type struc- ture (structure formed after melting of ice lenses) and with numerous small carbonate concentrations in the pores. This sequence was formed due to eolian and low-

intensity colluvial processes and was subjected to freezing under conditions of a cold periglacial climate [25].

On the slope (pit 4) and at the bottom of the buried paleohollow (pits 1—3), at a depth of 3.5—5.5 m from the surface, an interglacial paleosol is preserved and can be traced along the catena (Fig. 2c). This paleosol consists of the A_{pyr}—Ah—E—EB—Bt—C horizons; this sequence does not change, only the thickness of the horizons varies along the catena. In the thalweg zone (pit 2), the thickness of the humus horizons is greatest (50 cm), while in other pits it is about 25—35 cm. In pits 1 and 3, the thickness of the eluvial horizons E and EB is increased (30—40 cm). The depth of the upper boundary of the horizon Bt1 is 390—400 cm from the surface in pits 1—3; the thickness of the entire profile pits 1 and 3 reaches 160—185 cm (Figs. 2b and 2c). In pit 4 (paleoslope position), the Ryshkovo paleosol lies closer to the surface (305—383 cm), and the thickness of its profile is much lower (78 cm), which is typical for steeper parts of slopes. Upslope from pit 4, the depth of the Ryshkovo paleosol sharply decreases, and it gradually thins out: first, the humus-accumulative Ah horizon disappears, then, the eluvial E and clay-illuvial Bt horizons disappear.

Pit 3 (Fig. 2b). Depths are indicated from the surface; in brackets, depths of the soil horizons from the upper boundary of the Ryshkovo paleosol (the pyrogenic layer) are given.

Layer 7.1. Ryshkovo paleosol.

A_{pyr} (AO), 355—356/357, [0—1/2] cm. A thin wavy pyrogenic layer saturated with black charcoal remains of various sizes, including large charcoals; dark gray with brownish tint (10YR 3/3), silty sand loam, smeary (probably, this layer represents a burnt litter (AO) layer); in some places, the pyrogenic layer is overlain by dense silicon—carbonate concretions that possibly represent the remains of baked ash.

Ah, 357—375 [2—20] cm. Gray loam (10YR 4/3), porous, with inclusions of large charcoal; cryptogranular structure; massive, homogeneous, with an abrupt upper boundary and a clear wavy lower boundary.

AE, 375—380 [20—25] cm. Sandy loam, light gray (10YR 5/4), with siltans; fine pores; heterogeneous due to alternation of layers and lenses of lighter and more humified material, with brownish mottles; abundant charcoals of various sizes; clear boundary; the transition is seen from changes in the color and texture.

E, 380—397 [25—42] cm. Sandy loam; pale yellow with siltans (10YR 6/2) and darker intraped mass (10YR 6/6); granular to fine angular blocky structure; few charcoals; iron nodules; horizontal layering is seen as alternation of bleached and light gray interlayers (particularly, on the right wall of the pit); clear boundary; the transition is seen from changes in the color and texture.

EB, 397—420 [42—65] cm. Silt loam; light brown with brown intraped mass; fine angular blocky; less porous; peds are covered by clay coatings and immersed in siltan (bleached) material penetrating into the illuvial horizon; gradual boundary marked by changes in the color and texture.

Bt1, 420—450 [65—95] cm. Silty clay loam; dark; with clay coatings (10YR 3/6) on ped faces, somewhat lighter intraped mass (10YR 4/6), and bleached siltan material

(10YR 7/3); compound structure: angular blocky aggregates parting to granules; dark brown coatings on ped faces; few quartz grains covered with siltan material; manganic concentrations; gradual boundary marked by changes in the color and texture.

Bt2, 450—520 [95—165] cm. Silt loam, slightly dry, brown (10YR 4/6), with prismatic structure; the number of mangans increases; manganic concentrations are seen on ped faces along with clay coatings.

Bt3, 520—540 [165—185] cm. Carbonate-free loess, more homogeneous in the lower part; silt loam to sand loam; prismatic peds and walls of fissures are covered by ferruginous clay coatings; craNon-carbonate loess, in the lower part it becomes more homogeneous with a medium-to-light grain composition, the edges of large prisms and cracks are covered with clayey-ferruginous cutans. Color: cutans 10YR 8/6, intraped mass 10YR 8/8. Mangans are seen on plant roots. Abrupt smooth boundary; the transition is seen from changes in the color and the appearance of carbonates.

C, 540—600 [185—245] cm. Moscow (Saalian) loess. Heterogeneous, pale yellow (10YR 6/4) silt loam to sand loam; calcareous veins of up to 1 mm in diameter and cylindrical concretions (up to 5 mm) in large pores; brown manganic concentrations; fine porosity; abrupt textural boundary at a depth of 600 cm.

Paleogene sand; homogeneous; whitish pale yellow (10YR 8/2) to yellow with few brown ferruginous interlayers of horizontal and cross bedding.

The paleosol studied in the Taneyev Quarry is sharply differentiated into the Ah—E—Bt horizons and is identical to the Ryshkovo paleosol described in the Aleksandrovsky Quarry, where its age was determined as Mikulio Interglacial (MIS 5e) [24, 28]. At the base of the Bt horizon in the Ryshkovo paleosol, an OSL date is 127.4 ± 7.9 ka; in the overlying Seymsky loess, 115.2 ± 6.6 ka [39]. These dates indicate the duration of interglacial pedogenesis and coincide with the age determinations for MIS 5e (130/128—117 ka) based on glacier ice and ocean drilling data [36]. For the EB horizon of the Ryshkovo paleosol in the Taneyev Quarry (depth 405 cm), an OSL date is 123 ± 16 ka (quartz-based dating) and 136 ± 10 ka (feldspar-based dating), which is in good agreement with the age of the Mikulino interglacial.

The paleosol at the bottom of the paleohollow in the Taneyev Quarry (pit 3) consists of the Apyr(AO)—Ah—AE—E—EB—Bt1—Bt2—Bt3—C horizons with a total thickness of 185 cm. The thickness of the humus horizon is 25—30 cm; of the eluvial horizon, 15 cm. At the lower boundary of the EB horizon, there is a thin interlayer of dark brown loam sloping deep into the quarry wall; the presence of this interlayer suggests redeposition of other material under the impact of erosional—accumulative processes on the slopes of the paleohollow.

The three main horizons differ from one another in color, structure, and texture. and granulometric composition. The structure is platy to fine angular blocky in the AE horizon and coarse angular blocky and coarse prismatic in the Bt horizon. Soil aggre-

gates inherit the post-schlieren structure of the Moscow loess, in which the Bt horizon was developed. Pedofeatures are also differentiated: siltans are abundant in the E and EB horizons, and brown clayey coatings appear in the upper part of the Bt horizon; dark gray manganic concentrations are seen in its lower part.

The illuvial horizon is especially well developed; it has a thickness of up to 100−120 cm and consists of two to three subhorizons differing in the shape of soil aggregates and the clay content.

The eluvial and transitional horizons are gleyed. The humus horizon of the interglacial paleosol is thicker than that in the Aleksandrovsky Quarry. It is layered and bears the features of redeposition processes on slope. According to the micromorphological characteristics, the Ryshkovo paleosol can be classified as a surface-gleyed soddy-podzolic soil (Stagnic Albic Retisol (Siltic, Differentic)).

In the top of the soil,, there is an intensely charred layer (Apyr) 1−2 cm thick, saturated with charcoals as a result of a strong forest fire in the catchment of the hollow. Although charcoal particles are scattered throughout the entire thickness of the humus horizon, the larger ones tend to concentrate at the top, within the AO horizon, forming dark gray to black mottles. Below, there are lenses (1−2 cm in thickness and up to 10−20 cm in length) of reddish orange (burnt) loam that changed its color being exposed to fire.

The soil profile in the edge part of the paleohollow is considerably eroded. Within a distance of 10−15 m from the paleohollow, the humus, eluvial, and transitional (EB) horizons successively disappear, and the illuvial (Bt) horizon is preserved only fragmentarily, being included in the profile of the Holocene soil.

Micromorphological observations indicate that the Apyr layer is structureless; it consists of brown organic matter that has lost its cellular structure, charcoal dust, and grains of the mineral skeleton, mainly quartz grains of fine sand and coarse silt fractions (Fig. 3a, red arrows). In the areas of concentration of charcoal particles (Fig. 3a, upper left corner), scattered grains of sparite are visible; in some places, they compose carbonate pedofeatures. Sparite grains are associated precisely with charcoal inclusions (Fig. 3b). Carbonates are similar to pyrogenic calcite, which is formed during the combustion of large quantities of organic (plant) mass [1, 13]. There are also Fe−Mn concentrations on top of the calcified charcoal−plant mass: shapeless, or stripe-shaped and dendritic (Fig. 3a, green arrow).

The AO horizon, 355−356/357 or [0−1/2] cm, contains a significant amount of black charcoal dust, as well as a brown mass of unburned and heavily decomposed plant material occurring in the form of thin discontinuous layers. There is also a silty clay material of pale yellow color (Fig. 3c). Carbonate-free microzones are observed in the horizon (Fig. 3d, cen-
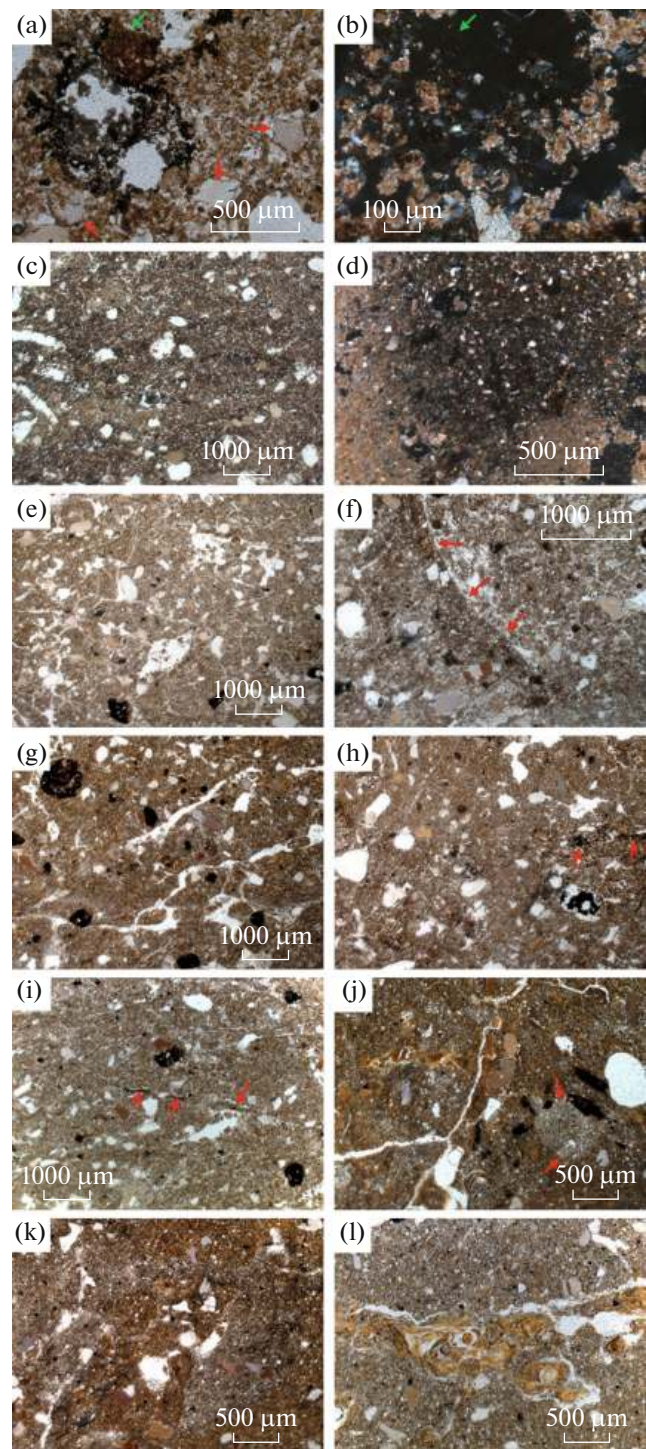

Fig. 3. Microfabrics of the MIS 5e paleosol horizons in the Taneyev Quarry. Explanations are given in the text. Only photos (b, d) were taken with the analyzer.

ter); carbonates are isolated in the form of micritic concretions or nodules in the fine mass (Fig. 3d, left edge and lower right corner). The horizon is structureless, it contains a network of root and earthworm passages, and casts of small soil animals in the pores (Fig. 3c).

The Ah horizon, 357(360)−375 or [3(5)−20] cm, is heterogeneous; it contains carbonaceous inclusions in the pores, sometimes in the form of discontinuous microlayers. In individual microzones, a post-schlieren structure (subparallel platy peds) is clearly seen. Microzones with a distinct granular structure and the presence of mesofauna casts are present in the pores (Fig. 3e). Carbonates are confined to biogenic pores and are represented by large needle-shaped crystals or by a thin layer of calcified root cells. The soil mass is heterogeneous in color with alternation of browner and grayer microzones (Fig. 3f, center, arrows).

The AE horizon, 375−380, [20−25] cm, demonstrates a clear network of subparallel pores−cracks dividing the soil mass into platy peds; bleached microzones—siltans—are clearly visible in the soil matrix (Fig. 3g, gray stripes on a rusty background); in some loci, siltans and humus−iron−clay coatings occur nearby. There are also many Fe−Mn concentrations scattered in the soil mass. In biogenic pores, carbonate coatings and charcoal particles are present sporadically in significant amounts (Fig. 3h). The soil mass is heterogeneous: microzones more or less colored with iron oxides and differently compacted are irregularly intertwined (Fig. 3h, lower and upper halves, respectively). Along the boundary between different materials, thin layers of charcoal dust are seen (Fig. 3h, arrows) marking different deluvial layers.

The E horizon, 380−397 [25−42] cm, is characterized by a pale yellow color; the main mass is not colored with iron hydroxides; the latter are concentrated in small (<0.5 mm) isolated rounded Fe−Mn punctuations; concentrations of charcoal dust are arranged as very thin interlayers (Fig. 3i, arrows). In the pores and in the soil matrix, accumulations of bleached quartz grains are seen. Carbonate concretions are found sporadically; the main soil mass is carbonate-free. The material is heterogeneous, with clearly visible microlayering; bleached skeletans are clearly visible along layer boundaries in some places.

The EB horizon, 397−420 [42−65] cm, leaves a double impression. On the one hand, bleached microzones of finely dispersed mass are well developed, but they often have unnaturally smooth boundaries (Fig. 3j, arrows), and intrusions of more clayey brown material are clearly seen. On the other hand, there are microzones with brown clayey and humus−Fe−clayey coatings and Fe−Mn nodules (Fig. 3j, center and left part). In these clayey microzones, there are inclusions of coarser grained iron-free material of irregular shape; the soil mass is broken by the network of fissures that cut both brown and light-colored fragments.

In the Bt1, 420−450, [65−95] cm and Bt2, 450−520, [95−165] cm horizons, brown silty clay material alternates with gray silty material (Fig. 3k), the latter being similar to the material of the Ah−EB horizons; a more clayey brown material could be seen in small quantities in the overlying EB horizon. The brown material contains many ferruginated clayey coatings; their number and thickness reach a maximum in the profile. the coatings display several stages of accumulation (Fig. 3l). From the top to the bottom of the illuvial part of the profile, the number of Fe−Mn concentrations increases, and their color becomes increasingly darker. The stipple-speckled b-fabric predominates; in some places, the cross-striated b-fabric is seen. This material differs from the material of siltans; it represents a mixture of silty and more clayey material. Cryogenic sorting of the material is also noted: grains of coarse sand size are concentrated in the pores, and are sometimes covered with ferruginous clayey coatings.

In the lower Bt3 horizon. 520−540, [165−185] cm, micromorphological features of the lithogenic matrix are seen from the similarity in size and shape of grains of the mineral skeleton, the presence of glauconite grains, and clear post-schlieren structure of the groundmass, which is also seen in the underlying Moscow (Late Saalian) loess (MIS 6). At the same time, there are significant differences: the Bt3 horizon is carbonate-free, except for the presence of rare elongated grains of lithogenic calcite; there are very thin, almost nonlayered and often fragmentary ferruginated clayey coatings in small pores and, less often, over the grains of mineral skeleton. In some places, these coatings are almost black because of the high content of Fe−Mn oxides; concentrations of Fe−Mn oxides are also present in the groundmass. Only a stipple-speckled type of b-fabric is present.

The Late Moscow (Saalian) loess is represented mainly by silty material with a noticeable proportion of virtually unrounded fine and medium sand particles. The post-schlieren structure of the material is clearly seen; pores−vughs do not have any covers, and the biogenic rounded pores (root passages) are occupied by cryptocrystalline calcite coatings. The optical orientation of the fine mass is not differentiated; in places of carbonate accumulation, anisotropic crystallites are seen. Dendritic patterns of Fe−Mn concentrations are observed carbonate coatings or in the groundmass. There are also recrystallized concentrations of sparitic carbonates. Among the grains of the mineral skeleton, there are glauconite grains and elongated and rounded lithogenic calcite grains indicative of the admixture of bedrock material (calcareous rocks of the Paleogene and Carboniferous ages) in the loess.

Physicochemical characteristics. *Particle-size distribution data* on the paleosol (MIS 5e) and the underlying Late Moscow loess (Fig. 4a) correlate well with the results of micromorphological description and clearly indicate the heterogeneity of the lithogenic matrix of the paleosol. In the upper part of the profile, including the EB horizon, the soil texture is sandy loamy with the high percentage of coarse silt fraction (53−57%); fine sand and fine silt fractions are present in approximately equal proportions, 11−16% each; the clay fraction content is about 3−8% with minimum values (about 3%) in the E and EB horizons. In the Bt1 hori-
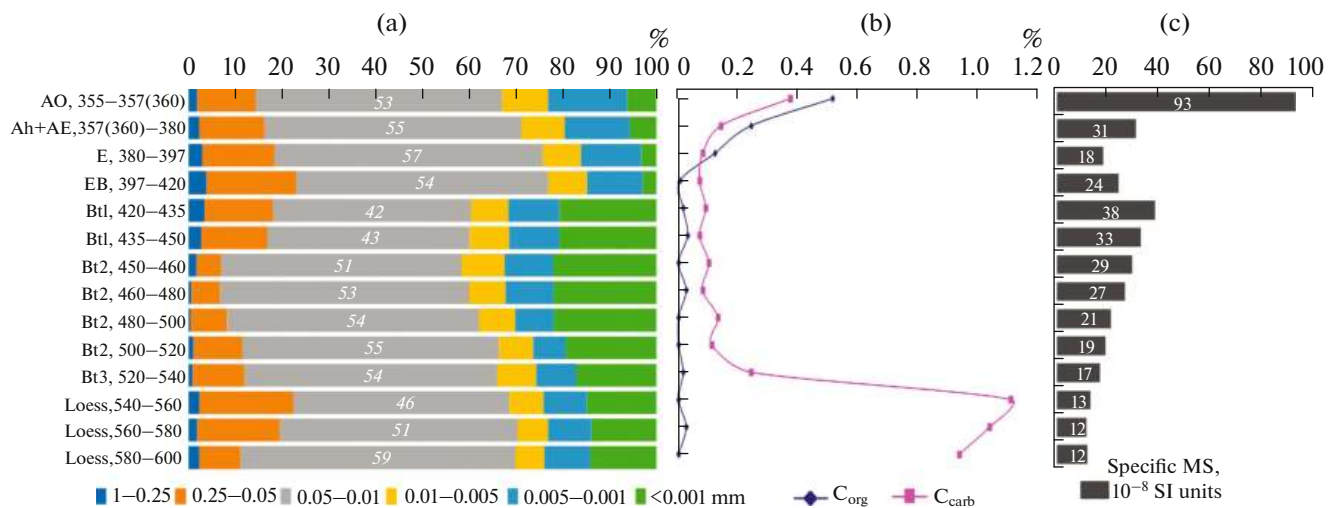
Fig. 4. Particle-size distribution (a), organic and carbonate carbon contents (b), and specific magnetic susceptibility (c) in the MIS 5e paleosol studied in the Taneyev Quarry.

zon, the content of coarse silt sharply decreases to 42–43%, and the clay content increases to 21–22%. The soil acquires the silty clay loamy texture, which is preserved down the profile to the lower boundary of the Bt3 horizon. Noteworthy is a noticeable decrease in the proportion of sand (both fine and, especially, medium sand) in the Bt2–Bt3 horizons. If we consider the set of Bt horizons of the MIS-5e paleosol, its layering in terms of the contents of clay and sand fractions is evident. Particle-size distribution in these horizons differs from that in the Late Moscow loess. In the loess, the texture is sandy silt loam, with a higher content of sand fractions and a lower content of clay.

The organic carbon (C_{org}) *content* varies from 0.5 to 0.2% in the upper humus horizon of the interglacial paleosol (Fig. 4b). In the EB horizon, it tends to zero. Slightly increased C_{org} contents alternating with zero values are seen in the Bt horizons of the paleosol and in the underlying loess.

The distribution of the carbon of carbonates (C_{carb}) is marked by a small peak in the pyrogenic layer Apyr (0.4%) decreasing to 0.1% in the Ah + AE horizons. It remains at the same level throughout the profile and sharply increases to 0.9–1.1% in the underlying loess (Fig. 4b).

Magnetic susceptibility shows a natural peak (up to 100×10^{-8} SI units) in the pyrogenic layer (Fig. 4c), where it is much higher than in the other paleosol horizons. Another increase in the magnetic susceptibility is seen in the Bt1 horizon (420–435 cm) and coincides with a sharp change in the soil texture and the character of soil microfabric In Moscow loess, the magnetic susceptibility is the lowest and does not exceed 13×10^{-8} SI units.

Spore-pollen analysis showed that the upper horizons of the buried paleosol contain pollen and spores,

but their concentrations are very low (Fig. 5). All the samples contained significant amounts of microscopic charcoal and phytoliths, including charred phytoliths.

In the AO horizon (355–357(360) or [0–3(5)] cm), pollen is practically absent (only single pollen grains have been found).

In the samples from the Ah horizon (357(360)–375 or [3(5)–20] cm), pollen of arboreous vegetation constitutes 53–72% of the total spectrum. The dominant species are pine and birch; spruce, oak, hazel, alder, and elm are found in small quantities (less than 5%). Pollen of herbs makes up 21–33% of the total spectrum; in addition to wild grasses, there are typical steppe species, such as wormwood (*Artemisia*) (up to 12%), Asteraceae (up to 3%), Chenopodiaceae, thalictrum, saxifrage, and grasses with large (>40 μm) pollen grains. Aquatic taxa included cattail (*Typha latyfolia)*, bur-reed (*Sparganium)*, and water-plantain (*Alisma)*. Spores are not numerous (7–13%) and are mainly represented by spores of sphagnum mosses.

In the AE horizon (375–380 or [20–25] cm), pollen of arboreous plants constitutes 57–65% of the total spectrum. The dominant species are pine (*Pinus sylvestris*) and birch (*Betula alba*) (about 20%). In addition, the presence of spruce (*Picea*) is noticeable (about 9%), and alder (*Alnus*) pollen constitutes 2–5% of the total spectrum. Oak (*Quercus*), linden (*Tilia*), and hazel (*Corylus*) were found sporadically. Herbaceous species make up 10–30% of the total spectrum, mainly due to grasses (Poaceae) and sedges (Cyperaceae); the remaining taxa are found sporadically. Among the spores, making up 11–25%, sphagnum mosses (*Sphagnum*) predominate; spores of clubmoss (*Lycopodium*) and ferns from the Polypodiaceae family and from the *Pteridium* and *Osmunda* general are found sporadically.
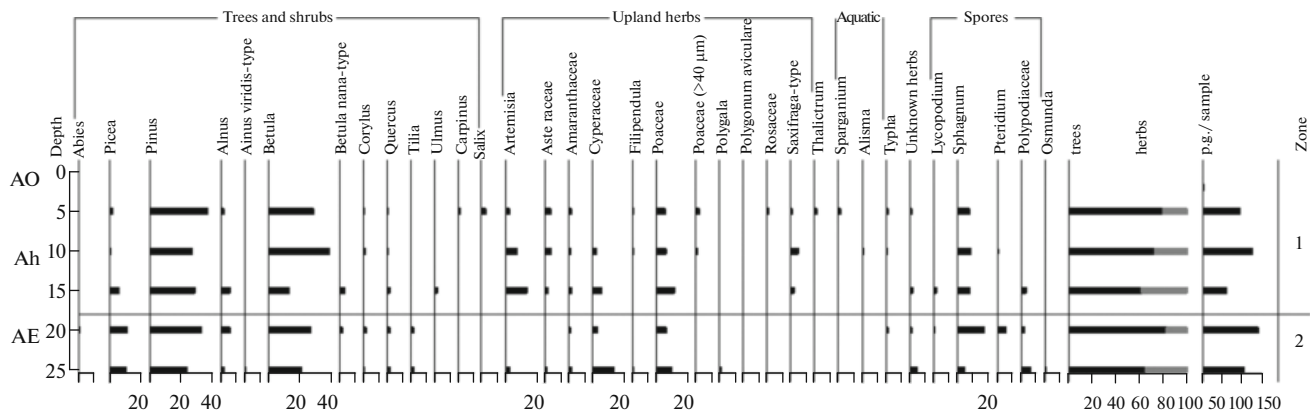
Fig. 5. Spore-pollen diagram of samples from humus horizons of the Ryshkovo paleosol in the Taneyev Quarry. The participation of pollen taxa is presented as a percentage of the total amount of pollen. The participation of spore taxa is presented as a percentage of the total of pollen and spores.

DISCUSSION

Based on macromorphological observations of the soil catena (pits 1–4), micromorphological descriptions, and data of physicochemical spore–pollen analyses, the Ryshkovo paleosol described in pit 3 consists of four differently aged strata representing the initial lithogenic matrix: (1) Bt3/BC–C; (2) Bt1–Bt2; (3) AE–E– EB; and (4) Apyr–AO–Ah.

Thus, though the Ryshkovo paleosol was generally formed on the Late Moscow (Saalian) loess, its lithological matrix did not remain unchanged due to the different history of interaction of eolian and slope (solifluction and colluvial) sedimentation, initial pedogenesis, and interglacial soil formation.

The Bt3 horizon in pit 3 and the BC horizon in pit 4 were developed from the Late Moscow carbonate loess (C). In the EB– Bt1–Bt2 horizons, a brown clayey mass without Fe–clay coatings is added to the silty loess. Starting from the E horizon upward, the soil is developed from the silty sand, in which the proportion of sand fractions reaches a maximum. In the Apyr–AO–Ah horizons, pyrogenic products (ash and charcoal, pyrogenic carbonates) appear in noticeable quantities in the silty sandy material. In terms of texture, these horizons do not differ from the underlying eluvial strata. Intrusions of heterogeneous material are visible in almost all horizons of the soil profile.

According to the particle-size distribution data, a lithological discontinuity is visible at the level of the upper boundary of the Bt1 horizon from a sharp (by seven times) increase in the content of the clay fraction and a decrease in the proportion of medium and fine sand; this decrease is especially noticeable in the Bt2 horizon (by three–six times) compared to the EB horizon. The lithological discontinuity is also seen between the base of the Bt3 horizon and the underlying loess.

The distribution of C_{org} has a clear maximum in the humus profile (AO–E horizons) and slightly increases in some parts of the Bt horizons and loess. The latter indicates the addition of not only clayey material but also material enriched in organic matter to the indicated horizons.

In the distribution of C_{carb}, the pyrogenic peak is clearly visible according to the chemical analyses and micromorphological observations [1], though this peak does not reach the values of the C_{carb} content in loess. This peak coincides with the peak in the magnetic susceptibility values: in the AO horizon, they are three times higher than in the soil profile as a whole. From the literature data, the enrichment of soils and cultural layers with the magnetic mineral fraction as a result of pyrogenic effects is well known [32, 33, 38].

The pollen spectra of the upper part of the humus profile (AO and Ah horizons) of the Ryshkovo paleosol reflect the vegetation of the final phase of the interglacial and transition to the early glacial: a combination of pine and birch forests with areas of tundra-steppe communities. In the lower part of the humus profile (AE horizon) there is less pollen of steppe grasses; in addition to pine and birch, there is pollen of spruce and broadleaved trees (linden, oak, elm, hornbeam), as well as spores of forest ferns and mosses. The spectra of this horizon are a mixture of pollen from different periods, formed as a result of soil and low-intense colluvial processes, so they do not reflect a specific type of vegetation. However, they give grounds to assert that more heat-loving spruce and broadleaved forests were present in the vegetation cover in the previous phases of the interglacial.

Interpretation. Comparison of OSL dates obtained for Ryshkovo paleosols in Aleksandrovsky (127 ± 8 ka at the base of the Bt horizon) and Taneyev (123 ± 16 ka in the EB horizon) quarries indicates high rates of sedimentation related to one sedimentation stage of the Late Moscow (Saalian) glaciation. It was preceded not only by the eolian accumulation of loess but also by the formation of small erosional landforms of two generations due to the degradation of permafrost [25].

The lower lithological discontinuity along the top of Bt3 horizon is probably associated with the boundary of the incision of the paleohollow (BSEL IIa) somewhat shifted upslope relative to the periglacial ravine (BSEL I). The upper erosional boundary at the level of the top of the Bt1 horizon is a consequence of the acceleration of sheet erosion at the very end of the Moscow Late Glacial during the transition to the interglacial.

The filling of the paleohollow and the formation of the lithogenic matrix for the Bt1 and Bt2 horizons reflect the highly dynamic paleogeomorphic conditions of the Moscow Late Glacial. Pits 1−3 are located in the paleohollow, where silty material slightly enriched in organic matter formed in the initial soils of the Moscow Late Glacial period came from the slopes and was deposited in the thalweg zone (this explains slight enrichment of some parts of the Bt horizons with the organic matter). This process can be called the cryogenic lateral or slope separation of fine earth according to its textural characteristics. The following explanation is offered. During the Late Valdai Glacial period, underdeveloped (initial) soils were formed in a periglacial environment described in loess sequences in the south of Moscow region [11, 16], in Voronezh region [19] and in some other areas [8]. In the section of the Upper Paleolithic site Kostenki 11 in Voronezh region, five such soils with profiles consisting of two horizons (AB or B and Bk, according to observations by S.A. Sycheva) were described. The character of their profiles and the specific fractured boundaries of the upper brown horizon suggest that these were initial soils rather than colluvial layers. The upper soil horizon was more ferruginous and clayey than the separating loesslike layers and could be slightly humified. Such soils reflect the warm phases of short-term climatic rhythms that took place during the highly dynamic time of the Late Glacial. During the pedogenic phase, initial soils were formed. Then, during the morpholithogenic phase, the material of their upper horizons was carried away and redeposited lower down the slope and/or accumulated in the bottoms of hollows or gullies and subjected to periodical freezing that created the lens-type (schlieren) structure in its lower part. After melting of ice lenses, cryogenic separation led to the alternation of sandy silt loam with more clayey interlayers; thus, the postschlieren structure was created.

The third lithogenic layer encompassing the EB−E−AE horizons was the result of eolian and slope sedimentation at the very end of the Late Moscow glaciation. In the Mikulino interglacial, these morpholithogenic processes continued, but without the participation of cryogenesis and initial soil formation.

The new eolian sediment of a coarser texture (coarse silt and fine sand are transported by wind easier than the clay fraction) accumulated during the final stage of the Late Glacial and at the beginning of the interglacial and was affected by the processes of zonal eluvial−illuvial pedogenesis under forest biocenoses. Podzolization and lessivage contributed to the vertical sorting of fine earth: depletion of the E and EB horizons in the clay fraction and clay enrichment of the Bt horizon. A single AE−E−Bt profile was formed with a series of transitional subhorizons marking the initial lithogenic textural differentiation and covering a significant thickness of loess sediments (from 1 to 2 m) depending on the energy of the interglacial climate, position in the micro- and mesorelief, and particular characteristics of the parent materials.

The AO−Ah horizons and, possibly, the very top of the AE horizon (the fourth lithological layer) were renewed during the interglacial period and contributed to the increased textural differentiation of the profile. After fires, which are a necessary mechanism for the functioning of forest ecosystems, the lateral transfer of fine earth during the Mikulino Interglacial periodically took place even on slightly inclined surfaces of uplands (with slope of more than 2°−3°. This was confirmed by the results of micromorphological and spore-pollen analyzes of the upper part of the Ryshkovo paleosol, especially in the bottoms of paleohollows with clear features of lithogenic (colluvial) layering. This layering did not have time to be "erased" by biogenic and chemical processes. This picture was also observed in the humus horizon of the Ryshkovo paleosol in the Aleksandrovsky Quarry [28]. The products of slope transport during the interglacial period accumulated at the footslopes or in newly formed depressions (ravines, balkas, hollows) thus composing interglacial soil−sedimentation archives [27].

In the fourth layer, traces of fast processes characteristic of the very end of the interglacial and even the beginning of the early glacial are present: thin post-schlieren structure, numerous traces of repeated forest fires (charcoal particles, siliceous−carbonate nodules, ashes, burnt loam material). According to the spore-pollen spectrum, the appearance of tundra-steppe communities can be assumed.

Thus, on the basis of the stratigraphic and catenary approaches, it has been established that the history of the lithogenic basis of the future Ryshkovo paleosol began in the Late Moscow Glacial with the deposition of loess (pits 3, 4) and the formation of periglacial ravines (pit 1).

History of the formation of the lithogenic matrix of Ryshkovo paleosol (four strata) includes the following stages of morpho-litho-cryo-pedogenesis:

(I) Formation of the parent rock of the lower strata (C−BC−Bt3) in the Moscow Late Glacial:

(1) Accumulation of loess (the first layer), its freezing and formation of ice lenses (schlieren structure) together with cryogenic separation of particle-size fractions of the loess material.

(2) Formation of initial soils (slight textural differentiation).

(3) Degradation of permafrost and formation of periglacial ravines (BSEL I): incision and rapid filling with colluvial loam forming a layered material.

(II) Accumulation of the second sediment layer (parent rock for the Bt2 and Bt1 horizons in the second half of the Late Moscow Glacial:

(4) A new stage of loess accumulation by eolian and deluvial processes.

(5) Formation of initial soils.

(6) A new stage of incision and the formation of a paleohollow (BSEL IIa) in the marginal part of the periglacial ravine.

(7) Gradual filling of the paleohollow with redeposited material from the initial paleosols, cryogenic separation of the material, and formation of a layer with a heavier texture—the lithogenic base of the upper part of the illuvial horizons.

(III) Textural differentiation with the periodic addition of new eolian and colluvial fine earth at the very end of the Late Moscow Glacial and the formation of lithogenic matrix for the EB−E−AE horizons as a result of eolian redeposition, post-fire soil erosion, and biogenic turbation during the interglacial. At the beginning of the thermochron, the Ryshkovo paleosol with the Ah−AE−EB horizons was renewed and maintained even on steeper slopes, although it was significantly reduced in thickness (pit 4). This was the main period of the formation of a texturally differentiated profile with preservation of the paleohollow (Mikulino BSEL IIb inherited from BSEL IIa). The lithogenic matrix of these horizons differed from the lithogenic matrix of Bt horizons in a coarser texture due to the absence of permafrost and cryogenic separation of coarse grains, as well as due to the addition of eolian component.

(IV) Biogenic accumulation with the addition of lithogenic material as a result of turbation and the participation of erosion-accumulation processes in the interglacial—formation of the lithogenic base of the upper strata (AE−Ah−AO).

(V) Catastrophic fire resulting in the formation of the pyrogenic layer (Apyr) at the end of the interglacial.

Thus, it is necessary to distinguish between the genesis, time, and history of the formation of parent materials for different horizons (Bt, E, Ah) and the development of a single profile of interglacial soil.

In the Valdai (Würm, Weichselian, Vistula) Late Glacial, the parent material of the future illuvial and partly eluvial horizons of the modern Holocene soils was formed [34, 37]. During the Moscow Late Glacial, a similar situation occurred: a new geomorphic basis for interglacial landscapes (BSEL I and then BSEL II) was formed, and the parent material of the texturally differentiated Ryshkovo paleosol of the Mikulino Interglacial accumulated [26]. Not only eolian and deluvial sedimentation but also cryogenic, slope, and pedogenic processes took part in the formation of this material.

The soil profile as a unified system of paragenetic horizons—a zonal type of soddy-podzolic and gray forest soils—is exclusively a product of the interglacial. Before the interglacial, it was only a layered or hidden-layered loess sediment; it was transformed into the full-profile texturally differentiated zonal soil only during the interglacial. The soil differentiation into the A−E−Bt horizons also took place in the interglacial, which is confirmed by the presence of soddy-podzolic and gray forest soils on newly formed surfaces (on Holocene sediments of floodplains and in the bottoms of ravines), as well as by the degradation of the Early Holocene chernozems and their transformation into gray forest soils [3, 23, 31, 40].

The Ryshkovo paleosol studied in the Taneyev Quarry, like a similar paleosol in the Alexandrovsky Quarry, reflects the entire complicated history of soil formation, as well as important moments in the life of soils and landscapes at the very end of the Mikulino Interglacial and at the beginning of the Valdai Early Glacial. The upper part of the humus horizons of the Ryshkovo paleosol contains evident traces of severe forest fires, which probably took place in the area as a result of prolonged spring−summer droughts, especially catastrophic in pine−birch forests on slopes of rugged terrain. Biogeocenoses at the end of the interglacial could not survive such repeated cataclysms, not only as a result of severe erosion, which caused the denudation of soils in the catchment area and the burial of the Ryshkovo paleosol in the bottoms and on the slopes of paleohollows but also because of the significant cooling that soon occurred. These events have yet to be experienced in the future by the modern Holocene soils and landscapes.

CONCLUSIONS

A new concept for the formation of the lithological matrix of texturally differentiated soils of the Mikulino Interglacial is suggested. The OSL dates and the mechanism of formation of the parent material of the Ryshkovo paleosol of the penultimate interglacial (MIS 5e) and the Late Moscow loess have been determined. In pre-Mikulino time (Moscow Late Glacial), eolian sedimentation alternated with initial soil formation and cryogenic and slope processes of sediment transport and redeposition reflecting the structure of short-term climatic rhythms. During the cold and dry phases of the rhythms, silty sediments accumulated. During the cold and wet phases, colluvial and solifluction processes were the main agents of sediment transport of redeposition. During the warm phases, initial soils were formed, which were destroyed, and the products of their destruction were redeposited downslope. As a result, this led to the formation of three lithogenic strata at the beginning of the interglacial: the upper stratum of a coarser texture, the middle stratum of the heaviest texture, and the lower stratum of the silt loamy (loess) texture. On this three-member lithogenic matrix, the Ryshkovo paleosol with the Ah−

AE−E−Bt−BC profile was developed during the interglacial under the impact of biogenic and soil processes. During the interglacial, the system of upper horizons was regularly renewed. Although the processes of sheet erosion slowed down, they did not stop completely during the thermochron, which was reflected in the characteristics of the Ah and AE horizons.

The established mechanism of stable interglacial soil formation was irrevocably disrupted at the end of the thermochron under the impact of catastrophic fires. At this time, the fourth (biogenic) stratum Apyr−AO−Ah was formed. Subsequent accelerated erosion in the catchment and climate cooling led to the burying of the paleosol in depressions and geomorphic traps and its partial denudation on higher surfaces of the slopes and inter-ravine watersheds.

The proposed concept is a compromise between the soil and lithogenic hypotheses of the formation of texturally differentiated soils; it does not contradict each of them, but complements the previous hypotheses. It can be used to explain the genesis of the parent material (Late Valdai loess) and the textural differentiation of modern Holocene soils.

Results of the study of Ryshkovo paleosols in the particular pits and in the catena encompassing the slopes and the bottom of the paleohollow demonstrated the complexity of the paleoenvironmental situation during the Late Moscow Glacial, which was characterized not only by the increasing role of soil formation but also by the highly dynamic nature of eolian and cryogenic and slope processes.

ETHICS APPROVAL AND CONSENT TO PARTICIPATE

This work does not contain any studies involving human and animal subjects.

CONFLICT OF INTEREST

The authors of this work declare that they have no conflicts of interest.

REFERENCES

1. A. L. Aleksandrovskii, " Pyrogenic origin of carbonates: Evidence from pedoarchaeological investigations," Eurasian Soil Sci. **40** (5), 471−477 (2007). https://doi.org/10.1134/S1064229307050018

2. A. L. Aleksandrovskiy, "The Holocene evolution of the soil cover of the Russian plain," Eurasian Soil Sci. **28** (5), 20−32 (1996).

3. A. L. Aleksandrovskiy, "Phases and rates of soil evolution within river floodplains in the center of the Russian Plain," Eurasian Soil Sci. **37** (11), 1137−1146 (2004).

4. A. L. Aleksandrovskii, V. O. Targulian, A. E. Cherkinskii, and O. A. Chichagova, "New data on the age and evolution of soddy-podzolic soils on cover loams," Dokl. Akad. Nauk SSSR **310** (2), 454−457 (1990).

5. A. L. Alexandrovskiy, Yu. G. Chendev, and A. A. Yurtaev, "Soils with the second humus horizon, paleochernozems, and the history of pedogenesis at the border between forest and steppe areas," Eurasian Soil Sci. **55** (2), 127−146 (2022). https://doi.org/10.1134/S1064229322020028

6. V. M. Alifanov, L. A. Gugalinskaya, and I. V. Kovda, "On the history of soils in the center of the Russian Plain," Pochvovedenie, No. 9, 76−84 (1988).

7. Z. P. Antonova, L. G. Skalabyan, and L. G. Suchilkina, "Determination of humus content in soils," Pochvovedenie, No. 11, 130−133 (1984).

8. V. A. Golubtsov, Yu. V. Ryzhov, and D. V. Kobylkin, *Soil Formation and Sedimentation in the Selenga Midlands in the Late Glacial and Holocene* (Izd. Inst. Geogr. im. V. B. Sochavy, Irkutsk, 2017) [in Russian].

9. B. P. Gradusov, "Processes of differentiation of the solid phase of soddy-podzolic loamy soils. Chapter 2," in *Soil Formation Processes* (Pochv. Inst. im. V. V. Dokuchaeva, Moscow, 2006) [in Russian].

10. L. A. Gugalinskaya and V. M. Alifanov, "Morpholithopedogenesis and neotectonics," Eurasian Soil Sci. **28**, 25−37 (1995).

11. L. A. Gugalinskaya, V. M. Alifanov, and L. A. Fominykh, "Concept of soil profile formation in the humid region of the Russian Plain," in *Spatiotemporal Organization and Functioning of Soils* (Pushchino, 1990), pp. 83−92.

12. F. R. Zaidel'man, *Theory of Formation of Light Acidic Eluvial Soil Horizons and Its Applied Aspects* (KRASAND, Moscow, 2010) [in Russian].

13. A. A. Kazdym, L. N. Koryakova, A. A. Kovrigin, and N. A. Berseneva, "Petrographic and mineralogical study of the "ash pits" of the Pavlinova settlement (5th century BC, Kurgan oblast)," Mineral. Tekhnogeneza **4**, 198−203 (2003).

14. A. O. Makeev, "Hypothesis of the formation of the profile of loamy podzolic soils of the Russian Plain," Byull. Pochv. Inst. **32**, 21−25 (1983).

15. A. O. Makeev, *Surface Paleosols of Loess Watersheds of the Russian Plain* (Molnet, Moscow, 2012) [in Russian].

16. A. Yu. Ovchinnikov, O. I. Khudyakov, O. S. Khokhlova, and A. M. Makshanov, "Paleocryolithopedogenesis and evolution of soddy-podzolic soils of the taiga zone in the northeast of the East European Plain," Eurasian

Soil Sci. **56** (12), 1911−1924 (2023).
https://doi.org/10.1134/S1064229323602172

17. A. M. Prokashev, *Genesis and Evolution of Soils in the Vyatka and Kama Basin (according to Paleosol Data)* (Izd. Vyatskogo Gos. Gumanitarnogo Univ., Kirov, 2009) [in Russian].

18. A. A. Rode, *Soil Genesis and Modern Soil Formation Processes* (Nauka, Moscow, 1984) [in Russian].

19. S. N. Sedov, A. A. Sinitsyn, S. Yu. Lev, A. A. Bessudnov, A. N. Bessudnov, S. A. Sycheva, T. V. Romanis, V. S. Sheinkman, and M. A. Korkka, "Paleosols of the Upper Palaeolithic sites in the East European Plain reflect the environmental fluctuations of centennial to millennial scale during MIS 3 and MIS 2," Geomorfologiya **53** (5), 69−77 (2022).
https://doi.org/10.31857/S0435428122050157

20. I. A. Sokolov, "On the genesis, diagnostics and classification of soils with a texture-differentiated profile," Pochvovedenie, No. 11, 32−41 (1988).

21. I. A. Sokolov, *Soil Formation and Exogenesis* (Pochv. Inst. im. V. V. Dokuchaeva, Moscow, 1997) [in Russian].

22. I. A. Sokolov, A. O. Makeev, T. V. Tursina, M. P. Verba, and E. V. Kulinskaya, "On the problem of the genesis of soils with a texturally differentiated profile," Pochvovedenie, No. **5**, 129−142 (1983).

23. S. A. Sycheva, "Small climatic optimum and the Little Ice Age in the memory of soils and sediments of the floodplains of the Russian Plain," Izv. Ross. Akad. Nauk. Ser. Geogr., No. 1, 79−93 (2011).

24. S. A. Sycheva, "New data on the composition and evolution of the Mezin loess-paleosol complex in the Russian Plain," Eurasian Soil Sci. **31** (10), 1062−1074 (1998).

25. S. A. Sycheva, "Paleomefrost events in the periglacial region of the Russian Plain at the end of the Middle and Late Pleistocene," Kriosfera Zemli **16** (4), 45−56 (2012).

26. S. A. Sycheva, "Buried Mikulino−Valdai relief and watersheds evolution of the Middle-Russian highland during the Late Pleistocene," Geomorfologiya, No. 1, 88−105 (2007).
https://doi.org/10.15356/0435-4281-2007-1-88-105

27. S. A. Sycheva, P. R. Pushkina, A. A. Golyeva, O. S. Khokhlova, T. M. Gorbacheva, and I. V. Kovda, "Stages of development of the Ryshkovo pedolithocomplex as an alternation of favorable and extreme conditions in the Mikulino Interglacial (MIS-5e)," Eurasian Soil Sci. **57** (1), 114−127 (2024).
https://doi.org/10.1134/S1064229323602524

28. S. A. Sycheva, S. N. Sedov, M. A. Bronnikova, V. O. Targulian, and E. Solleiro-Rebolledo, "Genesis, evolution, and catastrophic burying of the Ryshkovo paleosol of the Mikulino Interglacial (MIS 5e)," Eurasian Soil Sci. **50** (9), 991−1009 (2017).
https://doi.org/10.1134/S1064229317090071

29. V. O. Targul'yan, T. A. Sokolova, A. G. Birina, et al., *Organization, Composition and Genesis of Soddy-Pale-Podzolic Soil on Cover Loams* (IGAN, Moscow, 1974) [in Russian].

30. V. D. Tonkonogov, *Clay-Differentiated Soils of European Russia* (Pochv. Inst. im. V. V. Dokuchaeva, Moscow, 1999) [in Russian].

31. Yu. G. Chendev, A. L. Aleksandrovskii, O. S. Khokhlova, M. I. Dergacheva, A. N. Petin, A. N. Golotvin, V. A. Sarapulkin, G. L. Zemtsov, and S. V. Uvarkin, "Evolution of forest pedogenesis in the south of the forest-steppe of the Central Russian Upland in the Late Holocene," Eurasian Soil Sci. **50** (1), 1−13 (2017).
https://doi.org/10.1134/S1064229322040068

32. W. H. Blake, P. J. Wallbrink, S. H. Doerr, R. A. Shakesby, and G. S. Humphrey, "Magnetic enhancement in wildfire-affected soil and its potential for sediment-source ascription," Earth Surf. Processes Landforms **31**, 249−264 (2006).
https://doi.org/10.1002/esp.1247

33. N. Jordanova, D. Jordanova, A. Mokreva, D. Ishlyamski, and B. Georgieva, "Temporal changes in magnetic signal of burnt soils—a compelling three years pilot study," Sci. Total Environ. **669**, 729−738 (2019).
https://doi.org/10.1016/j.scitotenv.2019.03.173

34. A. Kleber, "Cover-beds as soil parent materials in mid-latitude regions," Catena **30**, 197−213 (1997).
https://doi.org/10.1016/S0341-8162(97)00018-0

35. A. Kleber and B. Terhorst, "Mid-latitude slope deposits (Cover Beds)," in *Developments in Sedimentology* (2013), Vol. 66.

36. L. E. Lisiecki and M. E. Raymo, "A Pliocene-Pleistocene stack of 57 globally distributed benthic D18O records," Paleoceanography **20**, 1−17 (2005).
https://doi.org/10.1029/2004PA001071

37. A. Semmel and B. Terhorst, "The concept of the Pleistocene periglacial cover beds in central Europe: a review," Quat. Int. **222**, 120−128 (2010).
https://doi.org/10.1016/j.quaint.2010.03.010

38. D. V. De Sousa, M. J. Rodet, D. Duarte-Talim, W. G. Teixeira, A. Prous, B. N. Vasconcelos, and E. Pereira, "Linking anthropogenic burning activities to magnetic susceptibility: Studies at Brazilian archaeological sites," Geoarchaeology **38**, 89−108 (2023).
https://doi.org/10.1002/gea.21941

39. S. Sycheva, M. Frechen, B. Terhorst, S. Sedov, and O. Khokhlova, "Pedostratigraphy and chronology of the Late Pleistocene for the extra glacial area in the Central Russian Upland (reference section Aleksandrov quarry)," Catena **194**, 104689 (2020).
https://doi.org/10.1016/j.catena.2020.104689

40. B. Terhorst, "The influence of Pleistocene landforms on soil-forming processes and soil distribution in a loess landscape of Baden−Württemberg (south-west Germany)," Catena **41**, 165−179 (2000).
https://doi.org/10.1016/S0341-8162(00)00098-9

Translated by D. Konyushkov